Proceedings of the

Advanced Architectures in Photonics

September 21–24, 2014 Prague, Czech Republic

Volume 1

Editors

Jiri Orava

University of Cambridge Department of Materials Science and Metallurgy 27 Charles Babbage Road CB3 0FS Cambridge United Kingdom

Tohoku University WPI-Advanced Institute for Materials Research (WPI-AIMR) 2-1-1 Katahira, Aoba-ku 980-8577 Sendai Japan

Tomas Kohoutek

Involved Ltd. Siroka 1 537 01 Chrudim Czech Republic

Proceeding of the Advanced Architectures in Photonics http://aap-conference.com/aap-proceedings

ISSN: 2336-6036 September 2014

Published by **Involved Ltd.**Address: Siroka 1, 53701, Chrudim, Czech Republic Email: info@involved.cz, Tel. +420 732 974 096



This work is licensed under a Creative Commons Attribution 3.0 Unported License.

CONTENTS

Preface T. Wagner (Chairman)	
FULL PAPERS	
Innovative nanoimprint lithography S. Matsui, H. Hiroshima, Y. Hirai and M. Nakagawa	1
Nanofabrication by imprint lithography and its application to photonic devices Y. Sugimoto, B. Choi, M. Iwanaga, N. Ikeda, H. T. Miyazaki and K. Sakoda	5
Soft-mould imprinting of chalcogenide glasses T. Kohoutek, J. Orava and H. Fudouzi	9
Electric nanoimprint to oxide glass containing alkali metal ions T. Misawa, N. Ikutame, H. Kaiju and J. Nishii	11
Producing coloured materials with amorphous arrays of black and white colloidal particles Y. Takeoka, S. Yoshioka, A. Takano, S. Arai, N. Khanin, H. Nishihara, M. Teshima, Y. Ohtsuka and T. Seki	13
<u>Stimuli-responsive colloidal crystal films</u> C. G. Schafer, S. Heidt, D. Scheid and M. Gallei	15
Opal photonic crystal films as smart materials for sensing applications H. Fudouzi and T. Sawada	19
Introduction of new laboratory device 4SPIN® for nanotechnologies M. Pokorny, J. Rebicek, J. Klemes and V. Velebny	20
Controlling the morphology of ZnO nanostructures grown by Au-catalyzed chemical vapor deposition and chemical bath deposition methods K. Govatsi and S. N. Yannopoulos	
<u>Visible photon up-conversion in glassy (Ge₂₅Ga₅Sb₅S₆₅)_{100-x}Er_x chalcogenides</u> L. Strizik, J. Zhang, T. Wagner, J. Oswald, C. Liu and J. Heo	
POSTERS presented at AAP 2014	
Solution processing of As-S chalcogenide glasses T. Kohoutek	31
Ga-Ge-Sb-S:Er ³⁺ amorphous chalcogenides: Photoluminescence and photon up-conversion L. Strizik, J. Oswald, T. Wagner, J. Zhang, B. M. Walsh and J. Heo	32
Multi-wavelength and multi-intensity illumination of the GeSbS virgin film P. Knotek, M. Kincl and L. Tichy	33
Towards functional advanced materials based using filling or ordered anodic oxides supports and templates J. M. Macak, T. Kohoutek, J. Kolar and T. Wagner	34
Introduction of new laboratory device 4SPIN® for nanotechnologies M. Pokorny, J. Rebicek, J. Klemes and V. Velebny	35
Profile and material characterization of sine-like surface relief Ni gratings by spectroscopic ellipsometry J. Mistrik, R. Antos, M. Karlovec, K. Palka, Mir. Vlcek and Mil. Vlcek	
Preparation of sparse periodic plasmonic arrays by multiple-beam interference lithography M. Vala and J. Homola	
High-performance biosensing on random arrays of gold nanoparticles B. Spackova, H. Sipova, N. S. Lynn, P. Lebruskova, M. Vala, J. Slaby and J. Homola	
2. Opasio (a, 1.1. O. po (a, 1.1. O.	



Ga-Ge-Sb-S: Er3+ Amorphous Chalcogenides: Photoluminescence and Photon Up-conversion

Lukas Strizik^{1*}, Jiri Oswald², Tomas Wagner¹, Jihong Zhang³, Brian M. Walsh⁴ and Jong Heo³

- Department of General and Inorganic Chemistry, Faculty of Chemical Technology, University of Pardubice, Studentska 573, 53210 Pardubice, Czech Republic
- Institute of Physics of the AS CR, v.v.i., Cukrovarnicka 10, 16200 Praha, Czech Republic
- Division of Advanced Nuclear Engineering, Center for Information Materials, Department of Materials Science and Engineering, Pohang University of Science and Technology (POSTECH), San 31, Hyoja-dong, Pohang, Gyeongbuk 790-784, Republic of Korea.
- NASA Langley Research Center, Hampton VA 23681, USA.

*Corresponding author (E-mail: lukas.strizik@centrum.cz, Tel.: +420 466 037 000)

Abstract

We report on the compositional tuning in $(Ge_{25}Ga_{10-x}Sb_xSe_{65})_{99.5}Er_{0.5}$ amorphous chalcogenides (x=0.5,2.5) and 5.0 at%) to achieve the intense photon up-conversion emission starting from green spectral region as well as Stokes emission in near- $(\lambda \approx 1.5 \, \mu\text{m})$ and mid-infrared $(\lambda \approx 2.7 \, \mu\text{m})$ spectral region. Thermal stability and glass-forming ability were found to increase with increasing antimony content but the photon up-conversion emission in green spectral region exhibits an opposite trend because of the red shift in absorption edge. The spectroscopic properties of Er^{3+} ions in Ga-Ge-Sb-S glassy host matrix were studied on the basis of Judd-Ofelt theory. The calculated spectroscopic quality factor Ω_4/Ω_6 is approximately 4 higher value than in commercial YAG: Er^{3+} lasers. Emission cross-section $\sigma_6(E)$ of Er^{3+} : $4I_{132} \rightarrow 4I_{152}$ ($\lambda \approx 1.5 \, \mu\text{m}$) was calculated from absorption cross-section $\sigma_6(E)$ on the basis of McCumber theory. The optical gain coefficient G(E) was calculated as function of the relative population of the Er^{3+} : $4I_{132}$ and $4I_{152}$ manifolds. The high absolute values of the gain coefficient make studied materials interesting for lasing and light amplification. The photon up-conversion emission seems to be promising for example in lasers, sensors and detectors.

Introduction and Goals

Amorphous chalcogenides are attractive host materials for doping them with lanthanide (Ln³+) ions. The reason can bee seen in their unique properties such as broad transparency from visible to mid-liferard speakers and the control of the control host such as broad transparency from visible to mid-infrared spectral region, low phonon energy, high refractive index, high solubility of Ln³⁺ ions in chalcogenides containing Ga and their relatively easy preparation in form of bulks as well as thin films [1].

The aims of presented work were:

- 1) to achieve efficient photon up-conversion emission starting from green spectral region
 2) to achieve important near- and mid-infrared Stokes
- 3) to study thermal and spectroscopic properties
- of prepared samples.

 The pumping laser diodes used in this work operate at wavelegnths of 808, 980 and 1550 nm.
- Studied materials are potentially applicable for lasers, sensors and detectors, erbium doped fiber amplifiers (EDFA) and light detection and ranging (LIDAR) [2].

Experimental Details

The studied samples were synthesized by standard melt-quenching technique from high-purity elements in silica glassy tubes at 970 C for 24 h. The melt was quenched into water and annealed close to glass transition temperature T_g for 3 h.

CHARACTERIZATION METHODS

X-ray Diffraction (XRD) analysis

Confirmation of amorphous state of prepared samples. Bruker AXE D8-Advance, CuKα tube with secondary graphite monochromator.

Energy Dispersive X-ray (EDX) spectroscopy

Confirmation of chemical composition of prepared samples. Microprobe as a part of the SEM microscope JSM-5500 LV Jeol, IXRF System, detector GRESHAM Sirius 10.

Differential Scanning Calorimetry (DSC)

Study of thermal properties, i.e. glass transition temperature T_g and crystallization temperature T_c . Heating rate: 3 K/min, N_2 rate: 50 mL/min. Heating rate: *3 K/ TA Instruments Q2000

UV/Vis/NIR Spectroscopy

Record of absorption spectra providing the information about the $4f \leftrightarrow 4f'$ electronic transitions and about the fundamental absorption oglassy host matrix. Spectral range: 300–2500 nm, step: 2 nm. Double beam spectrophotometer Jasco V-570.

Spectroscopic Ellipsometry (SE)

Determination of dispersion of the refractive index. Spectral range: 300–2300 nm, step: 20 nm. Data were evaluated using the Cauchy [3] and Sellmeier [4] formula. The roughness of the samples was modelled using the effective medium approximation (EMA) according to Bruggemann [5] with 50 vol% of voids and 50 vol% of chalcogenide material. VASE*, LA Woolland Co. Inc. J.A. Woollam Co., Inc.

Photoluminescence (PL) Spectroscopy

Recording of emission spectra and measurement of time-dependent luminescence decay to determine the lifetimes τ. Spectral range: 400–5000 nm, Step: 0.5–2 nm. Pl. spectrophotometer with pumping lasers of λ_{ccc} = 808, 980, 1550 nm The variety of detectors such as PMT, InSb, InGaAs, HgCdTe, Ge were used. Measurements were performed at room temperature.

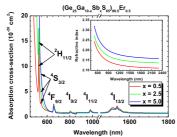
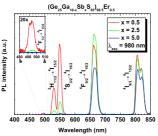


Fig.1. Absorption cross-section of the $\text{Er}^{3^{-1},4} 1_{152} \rightarrow {}^{25^{+1}} L_{o}$ transitions and spectral dispersion of the refractive index (Figure inset) in $(\text{Ge}_{25}\text{Ga}_{10-x}\text{Sb}_x\text{S}_{65})_{99,5}\text{Er}_{0.5}$ glasses.



ectra of (Ge₂₅Ga_{10-x}Sb_xS₆₅)_{99.5}Er_{0.5} glasses

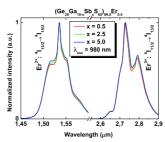


Fig.5. Stokes emission spectra of $(Ge_{25}Ga_{10-x}Sb_xS_{65})_{99.5}Er_{0.5}$ glasses at pumping wavelength of $\lambda=980$ nm.





Tab.2. Mean coordination number (MCN), glass transition temperature T_g , melting temperature T_m , thermal stability $\Delta T = (f_c - T_g)$ and glass forming ability $H_R = (T_c - T_g)(T_m - T_c)$ of $(Ge_{2r}Ga_{(0-r)}Sb_{S_c})_{pr_s}E_{G_s}$ glasses.

x (at%)	MCN	<i>T_g</i> (°C)	<i>T_c</i> (°C)	<i>T</i> _{au} (°C)	Δ <i>T</i> (°C)	H_R
x = 0.5	2.71	417	528	626	111	1.14
x = 2.5	2.69	383	508	575	125	1.88
x = 5.0	2.67	370	499	555	129	2.30

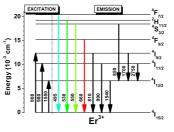
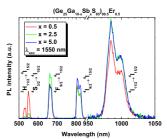


Fig.2. Energy level diagram nic transitions in (Ge₂₅Ga_{10-x}Sb_xS₆₅)_{99.5}Er_{0.5} glasses.



ectra of (Ge₂₅Ga ng wavelength of $\lambda = 1550 \text{ n}$

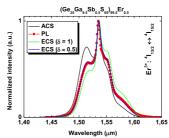


Fig.6. Absorption cross-section (ACS) and emission cross-section (ECS) spectra calculated via McCumber theory for the case of homogeneous ($\delta \approx 0.5$) broadening in $(Ge_2Ga_6g_5B_0, S_{6/5})$, $gEr_{0.5}$ glass. The red line (PL) is experimentally measured emission spectrum at pumping in $(Ge_{25}Ga_{9.5}Sb_{0.5}S_{65})_{99.5}Er_{0.5}$ experimentally measured er wavelength of $\lambda = 980$ nm.

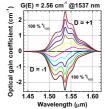


Fig.7. Calculated optical gain coefficient G(E) as function of the relative populations of Er^{3+} : $^4I_{15/2}$ and $^4I_{13/2}$ manifolds in $(Ge_{25}Ga_{9,5}Sb_{0.5}S_{65})_{99,5}Er_{0.5}$ glass.

Results & Discussion

Fig.1 shows the absorption cross-section spectra of studied samples with observed Er³⁺ intra-4*f* electronic transitions (see Fig.2). The absorption edge of samples exhibits a red shift with increasing antimony content. This results in increase of the refractive index as well. This behavior can be attributed to Clausius-Mossotti relation dealing with the atomic polarizability and dielectric function [6].

and detectric function [6]. Observed photon up-conversion emission bands were centered at wavelengths $\lambda \approx 495$, 530, 550, 660, 810 and 990 nm as show Fig.3 and Fig.4 for pumping wavelengths of 980 and 1550 nm, respectively. The up-conversion emission in the green spectral range is strongly affected by antimony content due to the red shift in absorption edge. The clear 1.5 and 2.7 μ m Stokes emissions are presented in the Fig 5 in absorption edge. The clear 1.5 and 2.7 μ m Stokes emissions are presented in the Fig.5. The emission cross-section σ_e of the Er³⁺: 4 1₁₃₂ \rightarrow 4 1₄₅₂ transitions was calculated from absorption cross-section σ_a via McCumber theory [7] for the cases of homogeneous and inhomogeneous broadening, see Fig.6. The case of inhomogeneous broadening leads to good match, between experimentally measured match between experimentally measured and calculated emission spectra. Optical gain coefficient G(E) calculated from σ_e and σ_a is shown in the Fig. 7 as a function of relative population of the Er³⁺: $^{4}I_{13/2}$ and $^{4}I_{15/2}$ manifolds [8], G(E) starts to be positive at $D \approx -0.4$ (≈ 30 %. [8]. G(E) starts to be positive at $D \approx -0.4$ (≈ 30 % 4) 4 1_{3/2}), i.e. at relatively low pumping power. The maximal value of G(E) is 2.56 cm⁻¹ at $\lambda \approx 1537$ nm. These results comparing to literature [8] make the studied samples promising for EDFA and lasing. Calculated Judd-Ofelt [9,10] parameters Ω_1 , Ω_4 , Ω_6 have tendency to decrease with increasing antimony content. The reason of this behavior can be seen in substitution of (CS). It observed the large Ω_1 with in substitution of $[GaS_{4/2}]$ tetrahedral units with $[SbS_{3/2}]$ pyramids. This substitution results in increase of glass forming ability and thermal stability of prepared samples as evident from $\Delta T = (T_c - T_g)$ and Hruby factor H_R . Spectroscopic quality factor Ω_s/Ω_c is approximately 4 higher than in commercially used VAG: Er³+ lasers [11]. Above mentioned results give a promise for using of the studied materials for EDFA, lasing, LIDAR, etc. The compositional tuning allows to find the trade-off between thermal stability and spectroscopic properties for specific applications. stability of prepared samples as evident from $\Delta T = (T - T)$ and Hruby factor $H_{\rm tot}$ applications

Literature

[1] A. Zakery and S.R. Elliott, J. Non-Cryst. Solids 330 (2003) 1

[2] L. Strizik, J. Zhang, T. Wagner, J. Oswald, T. Kohoutek, B.M. Walsh, J. Prikryl, R. Svoboda, C. Liu, B. Frumarova, M. Frumar, M. Pavlista, W.J. Park and J. Heo, J. Lumin. 147 (2014) 209.

[3] L. Cauchy Bull Des Sc Math. 14 (1830) 9

[4] W. Sellmeier, Ann. Phys. Chem. 143 (1871) 271.
[5] D.A.G. Bruggemann, Ann. Phys. 24 (1935) 636.

[6] R. Clausius, Die Mechanische Wärmlehre. Vol. II. 1879, Brunswick: Vieweg-Verlag; O. Mossotti, Mem. e Fisica di Modena

171 D.E. McCumber, Phys. Rev. A-Gen. Phys. 136 (1964) A954.

[7] D.E. McCulliner, *Phys. Rev. A-Gen. Phys.* **15** (1904) A959.
 [8] C. Koughia, M.G. Brik, G. Soundararajan and S.O. Kasap, *J. Non-Cryst. Solids* **377** (2013) 90.
 [9] B.R. Judd, *Phys. Rev.* **127** (1962) 750.

[10] G.S. Ofelt, J. Chem. Phys. 37 (1962) 511.

[11] D.K. Sardar, W.M. Bradley, J.J. Perez, J.B. Gruber, B. Zandi, J.A. Hutchinson, C.W. Trussel and M.R. Kokta, J. Appl. Phys. 93

Conclusions

We presented the compositional tuning of the $(Ge_{25}Ga_{10-x}Sb_xSe_5)_{95}Er_{0.5}$ amorphous chalcogenides (x=0.5,2.5 and 5.0 at%) allowing to find the trade-off between thermal stability and spectroscopic properties. The photon up-conversion emission was observed from green $(\lambda \approx 530,550$ nm) to near-infrared $(\lambda \approx 810,990$ nm) spectral region and it is strongly dependent on the antimony content. The substitution of $[GaS_{4/2}]$ tetrahedral units with $[SbS_{3/2}]$ pyramids results in increase of glass forming ability (H_R) and thermal stability (ΔT) however, it causes a dramatic red shift of absorption edge which results in low up-conversion emission intensity in the green spectral region. This substitution affects local environment around Er^{3+} site as is evident from Judd-Ofelt phenomenological parameters Ω_2 , Ω_4 , Ω_6 . The important near- ($\approx 1.5 \text{ µm}$) and mid-infrared ($\approx 2.7 \text{ µm}$) Stokes emission bands were also observed. The spectroscopic quality factor Ω_4/Ω_6 and the results of McCumber theory (σ_c , G(E), D) predicts these materials to be promising for EDFA and lasing at low pumping powers. The studied Er3+-doped amorphous chalcogenides are potentially applicable for up-converters, sensors and detectors, EDFA, LIDAR and lasers. The photoluminescence intensity and quantum efficiency can be probably further increased and controlled preparing these materials in glass-ceramic state or by their shaping into photonic crystals structures.

Acknowledgement

This work was supported by project CZ.1.07/2.3.00/20.0254 "ReAdMat - Research Team forAdvanced Non-Crystalline Materials" co-financed by the European Social Fund and the state budget of the Czech Republic and MEYS (Czech Republic), KONTAKT II, project no. LH11101 at the University of Pardubice, Czech Republic. The authors thank Roman Svoboda (University of Pardubice, Czech Republic) for DSC measurement















